

DETERMINATION OF THE GALAXY CLUSTER ORIENTATION USING X-RAY IMAGES BY FOCAS METHOD

S.Yu. Shevchenko¹, A.V. Tugay²

¹ Schmalhausen Institute of Zoology,
Bohdan Hmelnytskyi St., 15, Kyiv, Ukraine, *astromott@gmail.com*

² Astronomy and Space Physics Department, Faculty of Physics,
Taras Shevchenko National University of Kyiv,
Glushkova ave., 4, Kyiv, 03127, Ukraine, *tugay.anatoliy@gmail.com*

ABSTRACT.

In our work we considered orientations of bright X-ray halos of the galaxy clusters (mainly Abell clusters). 78 appropriate clusters were selected using data from Xgal sample of extragalactic objects in XMM-Newton observation archive. Position angles and eccentricities of these halos were calculated applying FOCAS method. No privileged orientations were found.

Keywords: Galaxies: clusters; X-rays: galaxies: clusters.

1. Introduction

One of the interesting tasks of the extragalactic astronomy is a search of dedicated directions in the galaxies and their clusters orientations. The catalog of Abell Cluster Objects (Abell et al., 1989) is the main catalog of galaxy clusters. It contains the most of closest and brightest clusters which are the most suitable for both optical and X-ray observations. Galaxy orientations in 247 rich Abell clusters were studied by Godlowski et al. (2010) and Panko et al. (2013) with corresponding statistical data analysis and simulations. Orientation of the galaxies from relatively small sample can be numerically described by the distribution of anisotropy parameter. This parameter was calculated for edge-on galaxies in Parnovsky & Tugay (2007) and for nearby galaxy groups in Godlowski et al. (2012). Galaxies orientation in the nearby groups was studied by Pajowska et al. (2012).

X-ray images of galaxy cluster halos could be easily approximated by ellipses, so they are well suitable to study such large-scale orientation. We use XMM-Newton archive based sample of X-ray extragalactic objects X-Gal (Tugay, 2012). In the previous work (Tugay et al., 2016) the orientation of 30 X-ray southern clusters from PF catalog (Panko & Flin, 2006) was determined using the method of image isophotes approximation by ellipses. In this work we

estimated orientation of the whole sky sample of X-ray brightest galactic clusters with more accurate FOCAS method (Jarvis & Tyson, 1981).

2. Method

Primarily X-Gal sample, comprised by about 5 000 objects was examined to find the brightest galaxy clusters. As a result 77 clusters were selected applying the precondition of the most right in X-Ray band. We used 1×10^{-11} - 110^{-12} mW/m^2 interval for the flux in 2-10 keV range. The major part of these objects (70%) turned out to be Abell clusters. Redshifts of our clusters are in the range from $z=0,02$ to $0,3$ (i.e. their distances reaches up to 1 Gpc). XMM-Newton imaging data (in FITS format) were retrieved from LEDAS (LEicesterDatabase and ArchiveService) and processed by XMM-SAS software. The next step was to use these data to calculate clusters X-Ray halo position angles (PA), eccentricities and their inaccuracies using FOCAS algorithm. Results are shown in Tables 1 and 2. The clusters in the tables are arranged by right ascension. For the obtained results we determined equatorial coordinates of the clusters orientation effective vector \vec{n}_A (Fig. 1). Vector \vec{n} points to the cluster center. Vector n_z points to Northern celestial pole (0, 0, 1). Cluster ellipsoid projection is given on the Fig. 2, where \vec{n}_A vector is the direction of the main axis of visible image. Direction of the third ellipsoid axis n_3 is not known. But it is known that the cluster ellipticity is insignificant and if there is measurable eccentricity of the cluster then it would be in the range of existing axis n_A and n_N . In general case, spatial orientation of the vector \vec{n}_3 is perpendicular to \vec{n}_A and hence within single-valued conversion of \vec{n}_3 it is possible to use vector \vec{n}_A instead. Hence vector \vec{n}_A was used to describe possible orientations of the cluster. It was determined from the following equations:

$$\begin{cases} n_{\vec{N}} \cdot [\vec{n} \times n_{\vec{Z}}] = 0 \\ n_{\vec{N}} \times \vec{n} = 0 \end{cases} \quad (1)$$

$$\begin{cases} n_{\vec{A}} \times \vec{n} = 0 \\ n_{\vec{A}} \times n_{\vec{N}} = \cos(PA) \end{cases} \quad (2)$$

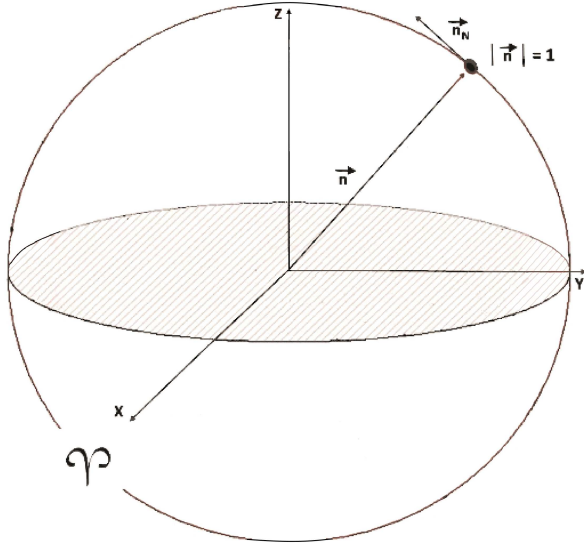


Figure 1: Cluster orientation directions.

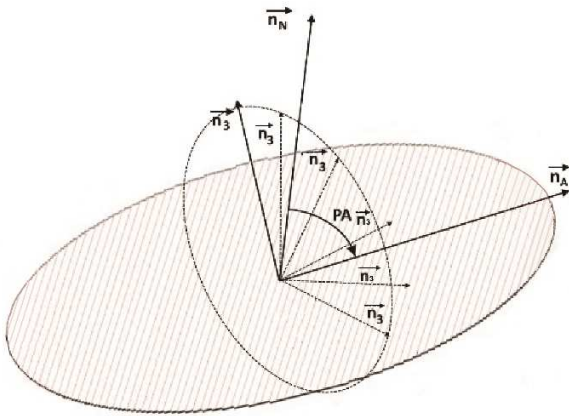


Figure 2: X-Ray halos orientation directions plane projections.

3. Results and conclusion

Orientation and Eccentricities of X-Ray halos are presented in Tables 1-2 and the distribution of the

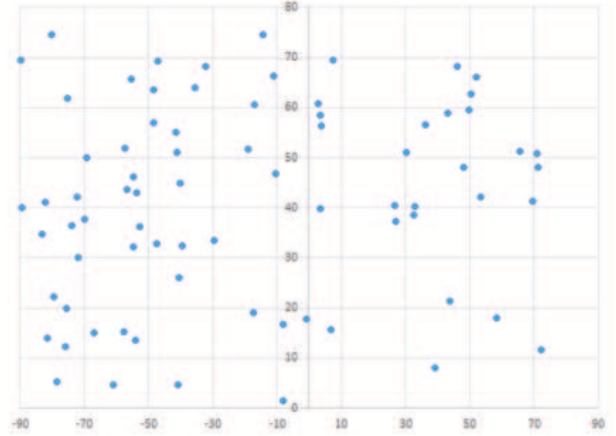


Figure 3: Distribution of the X-Ray halos orientation directions for RA and DEC.

\vec{n}_A orientation (RA, Dec) is given on Fig.3. To check possible anisotropy the range of the right ascension and declination of the \vec{n}_A was split into 10 degree intervals. Then using Kolmogorov's criterion we determined maximal mean deviations for clusters number in each interval and hence further verified probability of the clusters orientation anisotropy. Uniformity of the distribution was established using above Kolmogorovs criterion. Application of this criterion enables with probability up to 95% to accept hypothesis that Local Universe in the range up to about 1 Gpcs is isotropic. Further comparisons of the X-ray halos alignments and galaxies clusters orientation in optical band might be required and useful in the next works.

Acknowledgements. The authors are thankful to Elena Panko for discussions related to this work. This research retrieved data from NASA's Astrophysics Data System and LEDAS archive of XMM-Newton observations.

References

- Abell G.O., Corwin H.G., Olowin, R.P.: 1989, *ApJS*, **70**, 1.
- Godlowski W., Piwowarska P., Panko E., Flin P.: 2010, *ApJ*, **723**, 985.
- Godlowski M., Panko E., Pajowska P., Flin P.: 2012, *JPhSt.*, **16**, 3901.
- Jarvis J.F., Tyson J.A.: 1981, *AJ*, **86**, 476
- Pajowska P., Godlowski M., Panko E., Flin P.: 2012, *JPhSt.*, **16**, 4901.
- Panko E., Piwowarska P., Godlowska J., Godlowski W., Flin P.: 2013, *Ap.*, **56**, 322.
- Parnovsky S., Tugay A.: 2007, *JPhSt.*, **11**, 366.

Tugay A.: 2012, *Odessa Astron. Publ.*, **25**, 142.

Tugay A., Dylida S., Panko E.: 2016, *Odessa Astron. Publ.*, **29**, 34.

Table 1: Orientations and Eccentricities of X-Ray halos.

Name	PA	e
ACO 2700	25 ± 11	0.51 ± 0.2
ACO 119	110 ± 3	0.09 ± 0.01
ACO 122	84 ± 2	0.713 ± 0.327
ACO 2984	84 ± 1	0.52 ± 0.4
ACO 399	63 ± 15	0.31 ± 0.1
ACO 401	53 ± 1	0.39 ± 0.25
ACO 3112	71 ± 5	0.62 ± 0.5
ACO 3158	82 ± 4	0.212 ± 0.01
ACO S 384	38 ± 20	0.36 ± 0.25
CIG 0422-09	19 ± 1	0.079 ± 0.01
ACO 496	8 ± 3	0.2 ± 0.1
CIG 0451-03	71 ± 8	0.17 ± 0.02
MCXC J0528.9-3927	46 ± 39	0.28 ± 0.16
MCXC J0532.9-3701	88 ± 1	0.19 ± 0.14
ACO 3378	111 ± 20	0.45 ± 0.21
ACO 3391	107 ± 3	0.22 ± 0.04
ACO 3404	45 ± 2	0.47 ± 0.3
ZwCl 0735+7421	42 ± 11	0.15 ± 0.08
CIG 0745-1910	76 ± 2	0.17 ± 0.46
ACO 653	46 ± 3	0.36 ± 0.2
ACO 689	46 ± 34	0.14 ± 0.01
ACO 773	103 ± 5	0.37 ± 0.25
ACO 901A	41 ± 20	0.36 ± 0.27
ACO 907	45 ± 22	0.42 ± 0.3
ZwCl 1021+0426	35 ± 9	0.46 ± 0.4
ACO 1084	20 ± 6	0.51 ± 0.33
ACO 1201	25 ± 15	0.5 ± 0.2
CIG J1115+5319	66 ± 5	0.25 ± 0.02
ACO 1413	4 ± 2	0.63 ± 0.35
MCXC J1206.2-0848	59 ± 25	0.24 ± 0.17
ZwCl 1215+0400	144 ± 9	0.49 ± 0.15
ACO S 700	8 ± 3	0.07 ± 0.01
ACO 3528	10 ± 1	0.6 ± 0.4
ACO 1651	99 ± 3	0.35 ± 0.27
ACO 1656	73 ± 3	0.18 ± 0.1
ACO 1663	48 ± 39	0.3 ± 0.2
ACO 1664	157 ± 5	0.48 ± 0.25
2E 2975	60 ± 15	0.28 ± 0.25
1325-5737	45 ± 33	0.17 ± 0.1
ACO 3558	43 ± 16	0.47 ± 0.3
ACO 1750N	140 ± 25	0.379 ± 0.24
ACO 3560	26 ± 14	0.32 ± 0.27
ACO 3562	150 ± 29	0.31 ± 0.14
ACO 1775	136 ± 40	0.31 ± 0.23
ACO 3571	84 ± 2	0.3 ± 0.01
CIG J1347-1145	11 ± 6	0.15 ± 0.08
ACO 1835	10 ± 5	0.21 ± 0.16
ACO 3581	69 ± 7	0.2 ± 0.06
1419+2511	30 ± 3	0.45 ± 0.3
NGC 5718 Group	61 ± 2	0.22 ± 0.15
CIG J1504-0248	147 ± 17	0.1 ± 0.06
ACO 2050	141 ± 34	0.47 ± 0.25
ACO 2052	135 ± 6	0.48 ± 0.3
ACO 2051	64 ± 8	0.25 ± 0.03
ACO 2055	12 ± 12	0.31 ± 0.13
ACO 2063	8 ± 4	0.25 ± 0.06
ACO 2204	7 ± 5	0.087 ± 0.01

Table 2: The same as Table 1 for the last clusters.

Name	PA	e
ACO 3667	8 ± 8	0.76 ± 0.08
2MAXI J2014-244	9 ± 1	0.52 ± 0.45
ACO 3693	39 ± 23	0.12 ± 0.08
CIG J2129+0005	24 ± 1	0.5 ± 0.3
ACO 3814	65 ± 23	0.56 ± 0.27
2217-1725	71 ± 6	0.22 ± 0.2
ACO 3854	37 ± 22	0.51 ± 0.37
ACO 3856	39 ± 10	0.56 ± 0.31
ACO S 1101	121 ± 2	0.45 ± 0.3
ACO 3992	2 ± 2	0.37 ± 0.1
ACO 2597	37 ± 1	0.17 ± 0.05
ACO 4010	148 ± 4	0.148 ± 0.01
ACO 2626	156 ± 5	0.67 ± 0.06
ACO 2667	133 ± 27	0.403 ± 0.28
ACO 2670	132 ± 35	0.23 ± 0.14
ACO 13	60 ± 20	0.41 ± 0.1
0018-0053	149 ± 2	0.12 ± 0.05
CIG 0016+16	67 ± 24	0.18 ± 0.02

Table 3: Coordinate codes for clusters with long designations.

Name	Coordinate code
1RXS J132441.9-573650	1325-5737
2XMM J141830.6+251052	1419+2511
XMMXCS J221656.6-172527.2	2217-1725
2XMMi J001737.3-005239	0018-0053